



# PERFORMANCE OF PLATE TRANSDUCER HAVING DIFFERENT SURFACE CONDITIONS ON ELASTIC WAVE MEASUREMENT

Laxmi Prasad SUWAL<sup>1</sup>, Reiko KUWANO<sup>2</sup>,

**ABSTRACT:** Piezo-ceramic elements have been extensively used for measurement of elastic wave velocity in laboratory soil specimens. This paper presents a study of the flat shaped disk type piezo-ceramic transducer, so called Plate Transducer, on elastic wave measurement of geo-materials at mainly two types of surface conditions, plain surface and corrugated surface. A series of experiments was conducted to investigate effects of surface condition of transducer on the propagation of P and S wave in Toyoura sand and Hime gravel. The shear stiffness obtained from Plate Transducer measurements are compared with those from other techniques, including Trigger Accelerometer method and triaxial cyclic loading.

**Key Words:** Small strain stiffness, Wave measurement, Laboratory test

## INTRODUCTION

The stress-strain response of soil is highly non-linear. The stress-strain curve from the origin to the peak may be roughly grouped in two ranges; the small strain linear elastic range and the non linear elastic-plastic range. The maximum shear modulus at very small strain level is defined as small strain stiffness modulus and denoted by  $G_{\max}$  or  $G_0$ . The shear stiffness modulus decreases with increasing shear strain ( $\gamma$ ). The small strain stiffness is associated with strain amplitude of 0.001% or less. The stiffness, within this strain range is considered as elastic, recoverable and independent of the strain level (Tatsuoka and Shibuya, 1992; Arroyo et al., 2003). Several laboratory techniques have been developed to measure the small-strain stiffness. Stiffness measurement through exciting elastic wave on a specimen is becoming increasingly popular. The working principle for piezo-electric transducers is that it generates electric voltage when it is subjected to a mechanical disturbance or vice versa. The stiffness derived from elastic wave measurement is known as the dynamically measured stiffness and the stiffness, statically and dynamically measured are basically the same when measured strain level is properly taken into account. Various types of piezoelectric transducers are being used on the study of geo-materials on laboratory specimens, including the most popular Bender Element method which may be difficult to apply to undisturbed or cemented materials due to its protrusive nature. It was also reported that the dynamically measured stiffness by Bender Element is lower than statically measured stiffness for coarse grained materials possibly because of loosening introduced around the sensor (Wicaksono, 2009). Plate Transducer developed in our laboratory is a disk shaped piezo-electric transducer having flat surface, applicable to both P and S wave measurement. The surface of the Plate Transducer used in the previous studies was made to be corrugated to intend to create good contact between the tested material and the transducer (Mulmi, 2008, Suwal and Kuwano, 2009). In this study, the Plate Transducers with various surface conditions, including corrugated surface, sand paper surface

---

<sup>1</sup> Graduate Student, Department of Civil Engineering, University of Tokyo

<sup>2</sup> Associate Professor, Institute of Industrial Science, University of Tokyo

and flat plain surface, were employed, as shown in Figures 1 to 3, in order to clarify effects of surface condition on the wave measurement for coarse geo-materials.

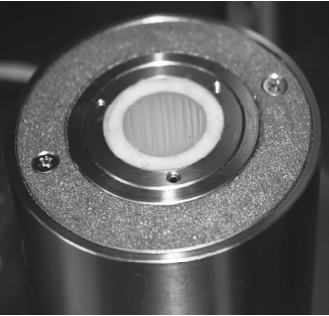


**Figure 1.** Plate Transducer having corrugated surface.

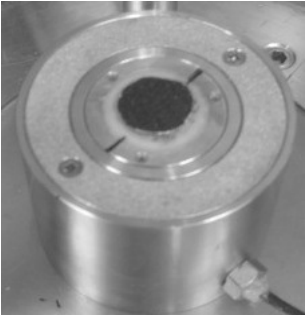


**Figure 2.** Plate Transducer having sand paper surface.

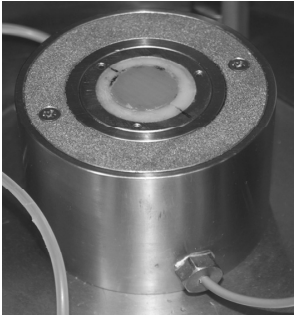


**Figure 3.** Plate Transducer having flat plain surface.

**APPARATUS AND METHODOLOGY**

In this study, small size, gear driven and strain controlled triaxial apparatus was used for performing experiments. The axial loading system consists of an AC servomotor and a reduction gear system, electro-magnetic clutches and brakes. The specimens of 75mm in diameter and 150mm in height were prepared by pluviating the material through air. The same procedure was applied for both Toyoura sand and Hime gravel. At first, the samples were set up at an isotropic stress state of 25 kPa, and then the stress was increased to 50, 100, 200 and 400kPa. Specimen was kept in each stress state for sufficient time period to dissipate the creep effect. 11 cyclic loadings with peak to peak strain amplitude of 0.001% were applied in vertical direction and another creep stage was maintained for conducting wave measurement. Deformations were measured by local deformation transducers (LDTs) developed by Goto et al (1991), which can measure local strain in higher accuracy and free from bedding errors. The picture of triaxial apparatus and LDT are shown in Figure 4 and Figure 5 respectively. The static stiffness is calculated based on the stress strain relation during small strain cyclic loadings. The schematic figure of typical plot of stress strain relation and stress path are shown in Figure 6 and Figure 7.

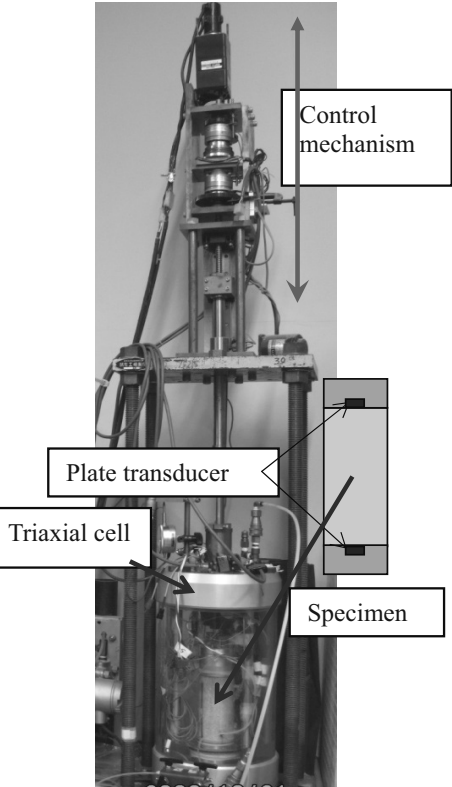


**Figure 4.** Triaxial apparatus

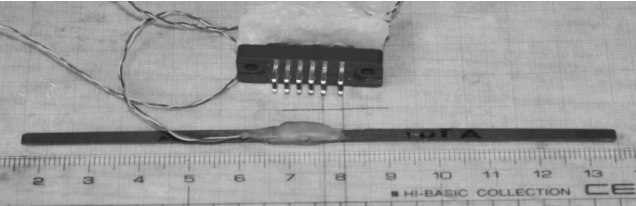


**Figure 5.** Local Deformation Transducer (LDT)

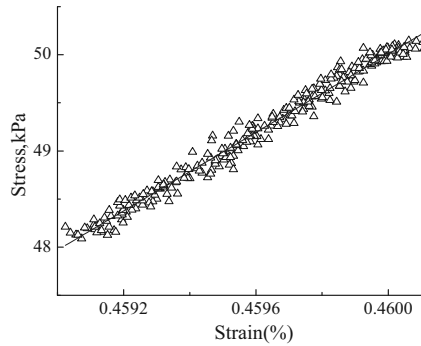


Figure 6. Stress-strain relation

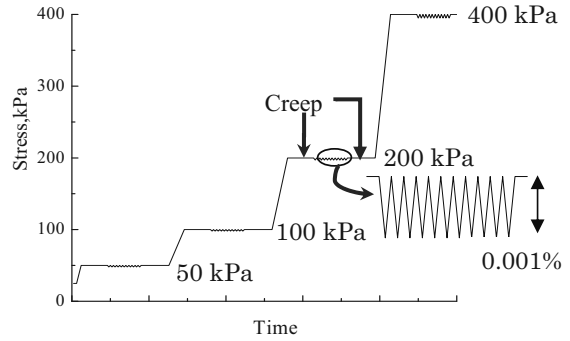


Figure 7. Stress path in test

### TESTED MATERIALS

Toyoura sand and Hime gravel were used in this study. Toyoura sand is fine-sized, uniformly graded sand; the source of this sand is Toyoura Beach of Yamaguchi prefecture, Japan. Hime gravel is poorly sorted, and the grain shape is angular. It was taken from Hime River, Otari, Kitazumi, Nagano prefecture, Japan. It is derived from sandstone, chert, granite, sill quartz etc. Pictures of these materials were shown in Figure 8 and Figure 9. Physical properties of the tested materials and gradation curves are shown in Table 1 and Figure 10 respectively.

Table 1. Physical and mechanical properties of tested materials

Physical and mechanical Properties	Toyoura sand	Hime gravel
Specific gravity, $G_s$	2.621	2.65
Maximum void ratio, $e_{max}$	0.946	0.709
Minimum void ratio, $e_{min}$	0.637	0.480
Mean Diameter, $D_{50}$ (mm)	0.196	1.716
Poisson's ratio	0.17	0.2

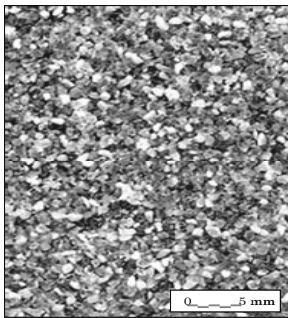


Figure 8. Toyoura sand

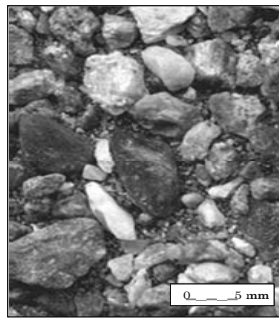


Figure 9. Hime gravel

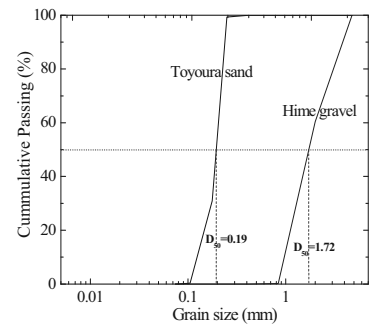


Figure 10. Particle size distribution

### SENSORS AND WAVE MEASUREMENT EQUIPMENT

The main objective of this study was to know performance and workability of Plate Transducer. Three types of Plate Transducers were used in experiments. P-type and S-type elements were purchased and developed as a sensor to suit in apparatus. The schematic figures of P-type and S-type elements are shown in Figure 11. In this study, thickness of 2mm and diameter of 20 mm P-type element and thickness of 5mm and diameter of 20 mm S-type element were used. PS-type element was developed by simply merging these elements in IIS Laboratory, which was used to measure P-wave and S-wave in a single specimen. The element is encapsulated in a metal housing and coating is applied on the surface for waterproof, as schematically shown in Figure 12. In this study, three patterns

of surface condition were used, including corrugated, flat plain and sand paper surface. In corrugated surfaced Transducer nearly 10 corrugation ditches were made by araldite. The ditches and cleavages were tried to make in triangular shape and eventually distributed in whole area of the transducer. The depth of ditches was found 1mm in average. In flat plain surfaced transducer, a thin layer of araldite was coated on transducer to protect from direct expose on material and make it waterproof. Sand paper of No. 40 was used for sand paper surfaced transducer, used for only trail tests (two tests). Signal for transmitting wave was generated by a digital automatic function generator manufactured by “Tektronix Co. Ltd.” It can produce a maximum peak to peak voltage of 10 V and is capable of producing twelve kinds of different waveforms at frequency ranges of 0.001Hz to 25MHz. An amplifier, NF-HAS 4014 was used to amplify the input signal generated by the function generator before feeding it into the transducer. The oscilloscope HIOKI 8855 MEMORY HiCORDER and HIOKI 8860-50 MEMORY HiCORDER were used to record and display waveforms of the transmitted and received signals. The features of the HIOKI 8860-50 MEMORY HiCORDER is given in Table 2.

Trigger Accelerometer method was developed in IIS in early 2000s. A pair of triggers is attached on the top cap of the apparatus and is actuated by a feeding signal by function generator, which gives an impact the whole area of the specimen. The propagated waves are sensed by the accelerometer attached on the lateral surface of the specimen. With the known distance between accelerometers, the velocity of wave can be calculated. The formulation of stiffness by this method is given in below (stiffness calculation section). The pictures of trigger and accelerometer are shown in Figure 13 and 14.

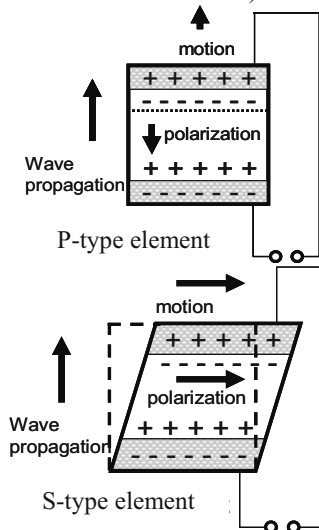


**Figure 11.** Schematic figure of P-type and S-type elements

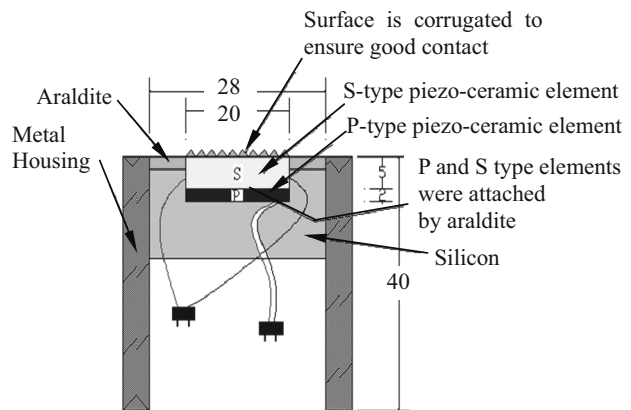


**Figure 12.** Structure of PS-type Plate Transducer

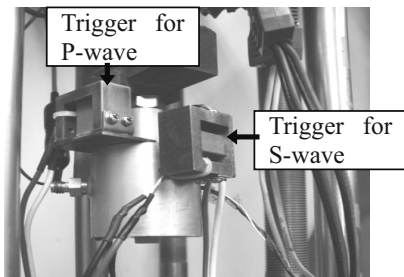


**Figure 13.** Trigger

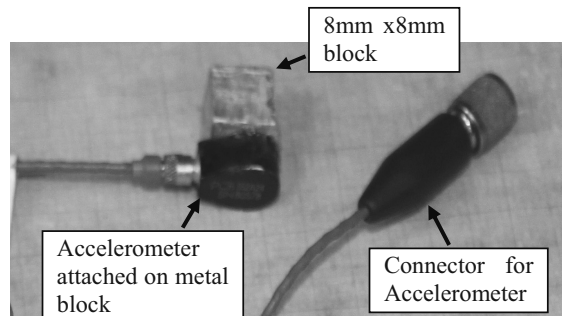


**Figure 14.** Accelerometer

**Table 2.** Features of Oscilloscope

No. of input units	Max. 4 units
No. of channels	Max. 16 analog channels (max. 64 channels with scanner unit) + 16 logic channels (standard configuration)
Measurement ranges	5mV to 20V/div, 12 ranges, (using the 8956), resolution : 1/100 of range
Max. allowable input	DC 400V
Frequency characteristics	DC to 10MHz
Time axis at memory function	5 $\mu$ s to 5 min/div, 26 ranges, sampling period : 1/100 of range, external sampling, dual time base possible
Memory capacity	12-bits $\times$ 32M-Words/ch (1ch at 8860-50, 2ch at 8861-50) to 2M-Words/ch (16ch at 8860-50, 32ch at 8861-50) *Memory capacity can be expanded 32 times.(Optional memory board)

**STIFFNESS CALCULATION**

Cyclic Young’s modulus ( $E_{cyc}$ ) was derived by fitting a straight line to the stress-strain curve. The stress-strain curves of 5<sup>th</sup> cycle and 10<sup>th</sup> cycle were utilized to analyze  $E_{cyc}$  (See Figure 6 and Figure7). The average results of 0.001% strain amplitude were obtained at each stress state. This stiffness is named as the statically measured stiffness modulus in this study. Stiffness by wave measurement was derived by general equation;

$$Stiffness = \rho V^2 \quad \text{-----} \quad (1)$$

Where,  $\rho$  is density of specimen and  $v$  is velocity of wave.  
 In case of Plate Transducer method, Plate Transducer was installed at center of top cap and pedestal. So the P-wave generated by Plate Transducer was considered as constrained wave involving no lateral deformation perpendicular to the direction of wave propagation (see Figure 15B). Constrained vertical modulus ( $M_{PT-P}$ ) could be achieved by Equation (2). The constrained modulus was then converted to the unconstrained modulus using the Equation (3).

$$M_{PT-P} = \rho V_{PT-P}^2 \quad \text{-----} \quad (2)$$

$$E_{PT-P} = \frac{M_{PT-P}(1-2\nu)(1+\nu)}{(1-\nu)} \quad \text{-----} \quad (3)$$

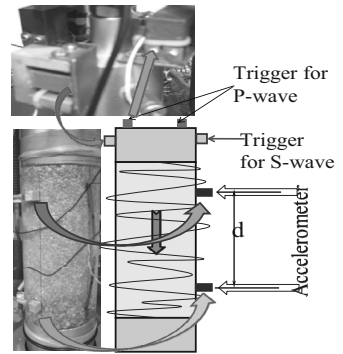
On the other hand, P wave in TA method is considered to be unconstrained wave propagation, as the triggers attached to a top cap generate vibration in a whole area of the specimen see Figure 15A), so that Equation (4) is applied to obtain Young’s modulus.

$$E_{TA-P} = \rho V_{TA-P}^2 \quad \text{-----} \quad (4)$$

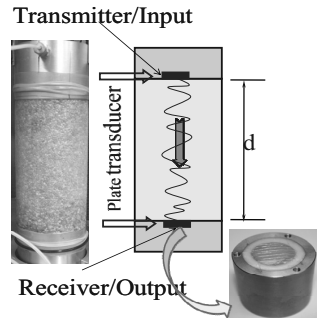
For getting shear modulus (G). The young’s modulus obtained was converted to G on the assumption that the material is isotropic using Equation (5);

$$G = \frac{E}{2(1+\nu)} \quad \text{-----} \quad (5)$$

Where,  $\nu$  is the Poisson’s ratio adopted as 0.17 (Hoque et al., 1996) for Toyoura sand and 0.2 (De Silva et al., 2004) for Hime gravel.



**A.** Unconstrained wave



**B.** Constrained wave

**Figure 15.** Unconstrained and constrained wave propagation.

For S wave velocities,  $V_s$ , measured by TA-S and PT-S are used to calculate  $G_{TA-S}$  and  $G_{PT-S}$  respectively by Equation (6).

$$G_{TA-S}, G_{PT-S} = \rho V_s^2 \quad \text{-----} \quad (6)$$

For the comparison of stiffness modulus of different dry densities with considering the effects of density or void ratio, the void ratio function proposed by Hardin and Richart (1963), as shown in Equation (7), was used in this study.

$$f(e) = \frac{(2.17 - e)^2}{1 + e} \quad \text{-----} \quad (7)$$

Where,  $e$  is void ratio.

## TEST DESCRIPTION

### TEST ON TOYOURA SAND

14 test results of Toyoura sand using Plate Transducer are presented. The list of experiments is tabulated in Table.3. 7 tests are with corrugated surface, 5 tests with plain smooth surface and 2 tests with sand paper surface. Figure 16 is the typical P-waveform obtained from T-02 with plain smooth surface (P-type plate) at 400kpa stress level of isotropic consolidation and Figure 17 is P-waveform obtained from T-06 with corrugated surface (PS-type plate). In calculation of P-wave velocity, it was assumed that the P-wave is faster than other wave and the first arrival point on time series was considered as the arrival of signal, which can be seen clearly in Figure 16 and 17. Figure 18 and Figure 19 is the typical S-waveforms obtained from T-14 and T-06 employing Plate Transducer having plain and corrugated surface condition at stress level 400kPa. The corrugated surface condition was assumed to be better for propagating S-wave by virtue the corrugation ditches increase the roughness and shear stress at interface of material and transducer. However, the plain surface seems to give equally good performance to the corrugated surface as shown in Figures 18 and 19. Amplitude of output signal voltage for tests, T-04, T-05, T-10 and T-12 are plotted against stress levels in Figure 20. Output voltage level depends on stress level and material density. For the plain surface, output voltage is proportional to the stress level and the pattern of waveform through corrugated surface is deviated from this trend. Plate Transducer with plain surface was actually difficult to apply for loose specimen at a stress level as low as 50kPa.

**Table 3.** List of specimens and conditions (Toyourea sand)

Test No.	Type of transducer	Surface condition	Specimen condition	Relative density (%)	Input Wave	Input voltage (V)	Input frequency(kHz)
T-01	P-type	Plain	Dry	95	sine	±50	7.8-31.25
T-02	P-type	Plain	Dry	74	sine	±50	7.8-31.25
T-03	S-type	Corrugated	Dry	92	sine	±100	7.8-31.25
T-04	S-type	Corrugated	Dry	95	sine	±100	7.8-31.25
T-05	S-type	Corrugated	Dry	67	sine	±100	7.8-31.25
T-06	PS-type	Corrugated	Dry	89	sine	±50	7.8-31.25
T-07	PS-type	Corrugated	Dry	68	sine	±50	7.8-31.25
T-08	PS-type	Corrugated	Saturated	91	sine	±100	7.8-31.25
T-09	PS-type	Corrugated	Dry	60	sine	±100	7.8-31.25
T-10	S-type	Sand paper	Dry	80	sine	±100	7.8-31.25
T-11	S-type	Sand paper	Saturated	80	sine	±100	7.8-31.25
T-12	PS-type	Plain	Dry	94	sine	±100	7.8-31.25
T-13	PS-type	Plain	Dry	92	sine	±100	7.8-31.25
T-14	PS-type	Plain	Dry	78	sine	±100	7.8-31.25

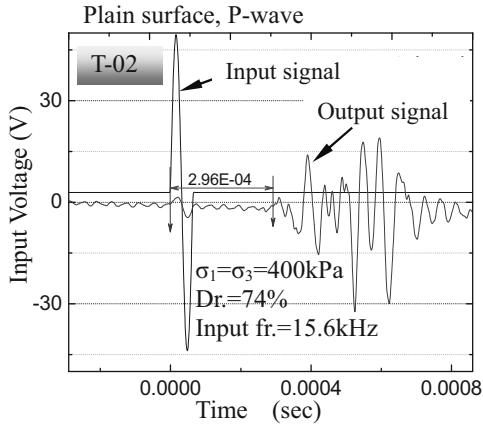


**Figure 16.** P-waveform by plain surfaced Plate Transducer on Toyoura sand (T-02)

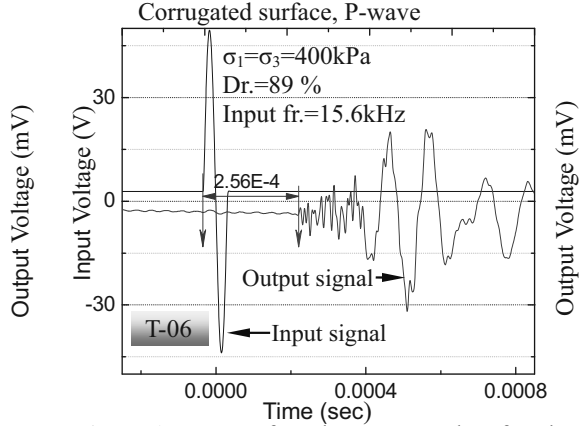


**Figure 17.** P-waveform by corrugated surfaced Plate Transducer on Toyoura sand (T-06)

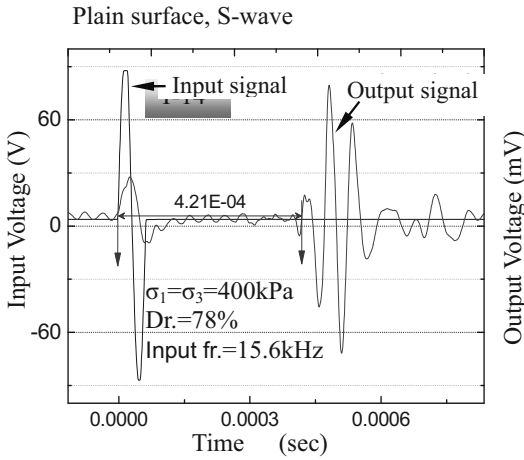


**Figure 18.** S-waveform with plain surfaced Plate Transducer on Toyoura sand (T-14)

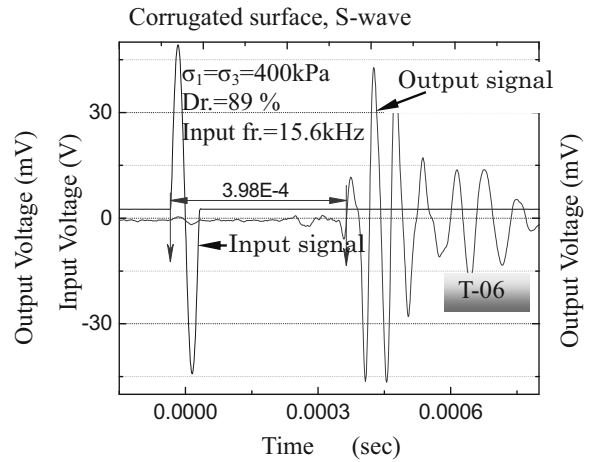


**Figure 19.** S-waveform with corrugated surfaced Plate Transducer on Toyoura sand (T-06)

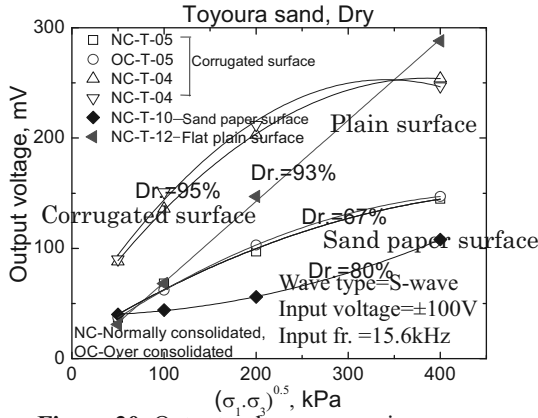


**Figure 20.** Output voltage comparison on Toyoura sand

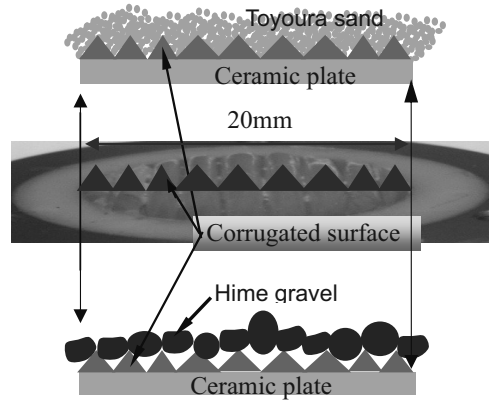


**Figure 21.** Contact conditions of Toyoura sand and Hime Gravel on corrugated surface.

### TEST ON HIME GRAVEL

6 tests were conducted on Hime gravel. Among them, 4 tests were conducted with the Plate Transducer having corrugated surface and 2 tests with plain surface condition. The list of tests is presented on Table 4. Even though well interpretable waveforms were generated at low stress level to high stress level, as shown in Figures 22 and 23 the corrugated surface may involve insufficient contact between transducer and material, as shown in Figure 21, since the ditches of the corrugated surface are relatively smaller than the grain size of materials.

**Table 4:** List of specimens and conditions (Hime gravel)

Test No.	Type of transducer	Surface condition	Specimen condition	Relative density (%)	Input Wave	Input voltage (V)	Input frequency (kHz)
H-01	PS-type	Corrugated	Dry	97	sine	±100	5.4-16.2
H-02	PS-type	Corrugated	Dry	94	sine	±100	5.4-16.2
H-03	PS-type	Corrugated	Dry	78	sine	±100	5.4-16.2
H-04	PS-type	Corrugated	Dry	98	sine	±100	5.4-16.2
H-05	PS-type	Plain	Dry	97	sine	±100	5.4-16.2
H-06	P-type	Plain	Dry	76	sine	±100	5.4-16.2

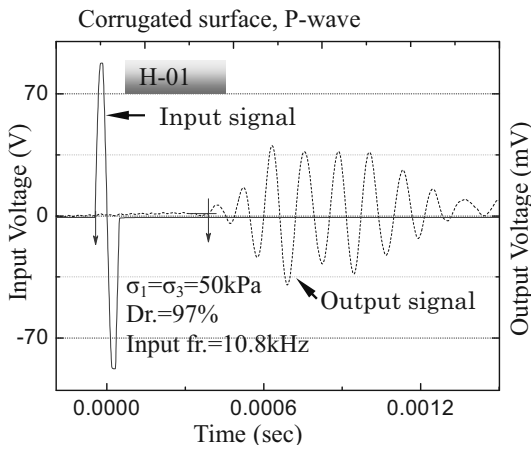


**Figure 22.** P-waveform with corrugated surfaced Plate Transducer on Hime gravel (H-01, 50kPa)

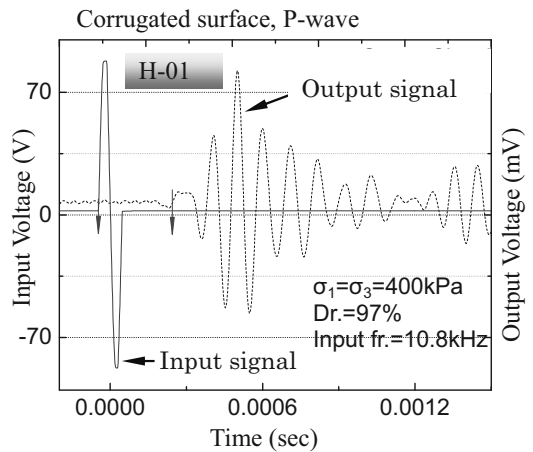


**Figure 23.** P-waveform with corrugated surfaced Plate Transducer on Hime gravel (H-01, 400kPa)



For the wave transmission and receiving, it is important to secure good contact between sensor and tested material and the surface condition is found to be the vital parameters. Density of the tested material and confining pressures are also governing factors. The measurement on looser specimen at lower stress level is therefore the severest condition. The plain surface showed good performance in tests at higher stress level, as shown in Figure 24, but was unable to provide the shear wave measurement at 50 kPa even for dense Hime gravel (H-05). The corrugated surface seemed to increase the roughness and facilitate to propagate the wave from transducer to materials at low stress level as compare to the plain surface condition, but the interpretation of received waveform for loose Hime gravel was not very easy, as shown in Figures 25 and 27. The output wave voltage linearly increases according to the stress level in plain surface condition, as shown in Figure 26, implying that the contact area of material at interface and angle of shear resistance are constant over the range of confining stresses. On the other hand for the corrugated surface, the interface condition seems to be more complicated, involving not only shear resistance at contact surface but also interlocking between material and corrugation etc.

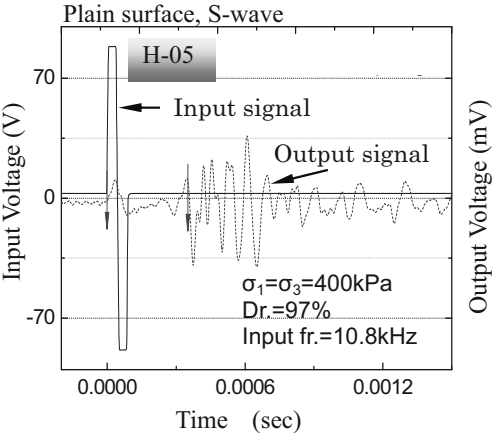


**Figure 24.** S-wave form with plain surfaced Plate Transducer on Hime gravel (H-05)

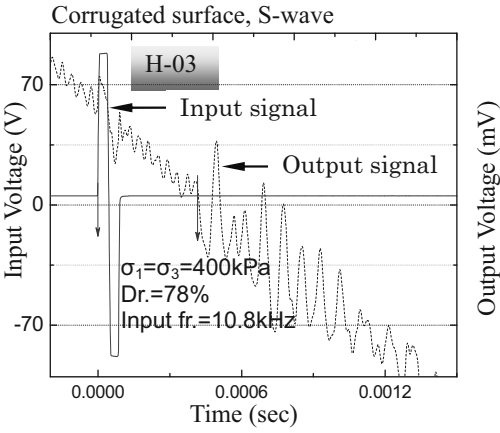


**Figure 25.** S-wave form with corrugated surfaced Plate Transducer on Hime gravel

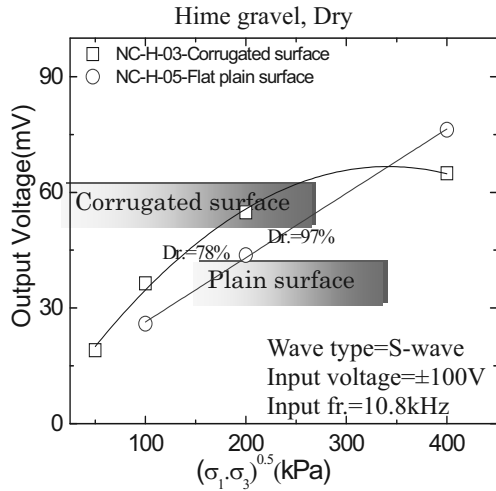


**Figure 26.** Output voltage comparison on Hime gravel

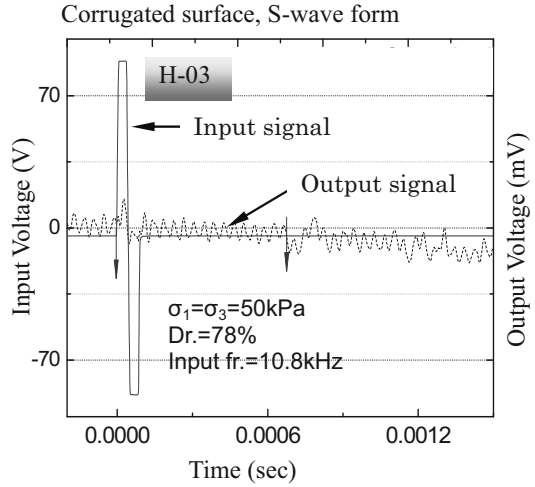


**Figure 27.** S-wave form with corrugated surfaced Plate Transducer on Hime gravel(H-03)

### TEST RESULT AND DISCUSSION

The determination of travel time of the wave is the most speculative and the most controversial issue in wave measurement. In this study, P-wave was analyzed without consideration of any disturbance as P-wave is faster than other waves. To identify the first arrival point in S-waveform, some disturbance in waveform due to the near field effect and other factors have been considered. In all cases travel time was determined as the time interval between rising the wave at first sensor to rising the wave in next sensor following the previous researches with Bender Element. In the received S-wave, there seemed to be some tendency according to materials. In case of Toyoura sand, S-waveforms were typically seen as some disturbances at first and the real signal was arrived with forming trough. The amplitude of first arrived signal has small amplitude and maximum amplitude follows this, then again decreasing gradually. In S-waveform of Hime gravel this behavior could not be sometimes observed. Typical traces of S-wave show the disturbances arrived at first and suddenly large amplitude of falling waveform was observed. In such a case, the beginning point of falling waveform is considered as the first arrival as shown as in Figure 28. In this study, the plate of 20mm in diameter was used. Mean diameters of Toyoura sand and Hime gravel are 0.2mm and 1.7mm respectively. Around 100 Toyoura sand grains are directly attached with the transducer where as in Hime gravel only 13 grains. By virtue of this configuration the amplitude of received wave is smaller for Hime gravel as compare to Toyoura sand. The arrival point of received wave for Hime gravel was not always clearly defined.

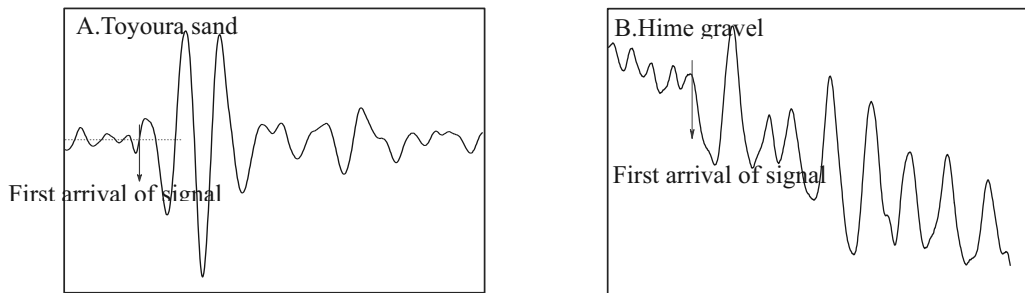


**Figure 28.** First arrival point in received wave for Toyoura sand and Hime gravel(S-wave)

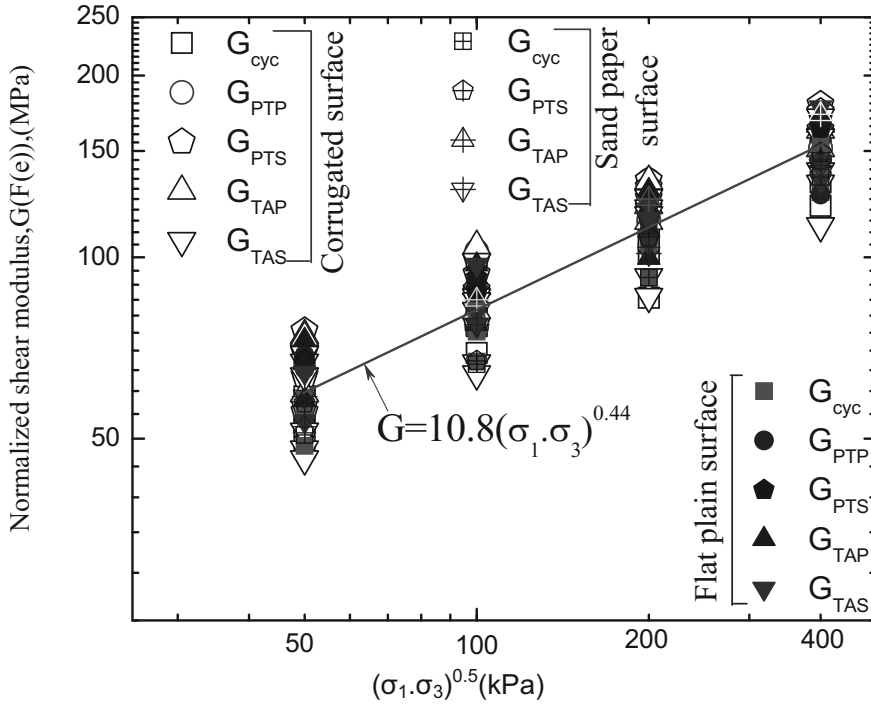


**Figure 29.** Results of Toyoura sand in various conditions.

As defined as above, the travel time was determined and the shear stiffness was calculated. The summary of all tests for Toyoura sand are shown in Figure 29 and Figure 30. In Figure 29, normalized shear stiffness are plotted with respect to the stress parameter in logarithmic scale showing the following relationship.

$$\frac{G}{f(e)} = 10.8(\sigma_1 * \sigma_3)^{0.44} \quad \text{-----} \quad (8)$$

Where,  $G(f(e))$  is normalized shear modulus in MPa and  $\sigma_1$  and  $\sigma_3$  are in kPa.

It seems that this Equation is unit dependent. General custom to express it in non-dimensional

$$\text{Equation as, } \frac{\left(\frac{G}{P_r}\right)}{f(e)} = A \left( \left(\frac{\sigma_1}{P_r}\right) * \left(\frac{\sigma_3}{P_r}\right) \right)^n \quad \text{-----} \quad (9)$$

In this Equation,  $P_r$  is reference stress level (pressure) and is considered 1kPa in here.  $f(e)$  is void ratio function proposed by Hardin and Richart, (1963) which was given in Eqn. (7).  $A$  and  $n$  are constant parameters. These parameters depend on the grain shape, grain size and other material properties Then

$$\text{Eqn. (8) can be expressed in non-dimensional form as, } \frac{G}{f(e)} = 10800(\sigma_1 * \sigma_3)^{0.44}$$

For the Toyoura sand,  $A$  was found as 10800 and  $n$  was 0.44 in this study. These values are determined considering all the tests results by all modes of measurements (Plate Transducer, Trigger Accelerometer and Cyclic loading method). Results of plain surfaced conditions lie inside those of corrugated surface condition in Figure 29, implying that plain surface provides stable results. In Figure 30, statically measured stiffness versus dynamically measured stiffness was plotted, making possible to evaluate the change in dynamically measured stiffness with respect to the statically measured stiffness

for corrugated and plain surfaced cases. Both corrugated and plain surfaced cases, the results were found following similar trend and no significant influence by surface condition. Generally, the dynamically measured stiffness is found higher than statically measured by approximately 20%.

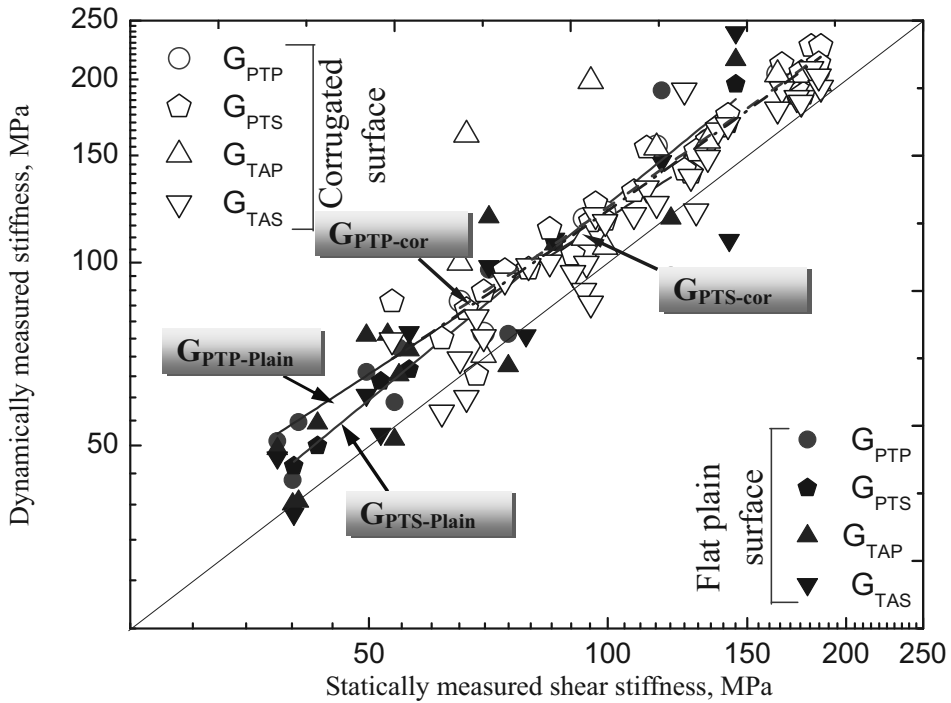


**Figure 30.** Comparison of dynamically and statically measured shear stiffness.

Figures 31 and 32 are the summary of the tests on Hime gravel. The statically measured stiffness (stiffness obtained from small cyclic loading) is considered not to be affected by the surface condition of Plate Transducer, as the strain is measured locally by LDTs which are free from bedding error. The stiffness by dynamic measurements seemed to be significantly influenced by type of contact surface between material and transducer. The stiffness by P-wave measurement with corrugated surface was noticeably lower than other mode of measurements. In plain surface cases, the value tended to higher than static result at higher stress level.

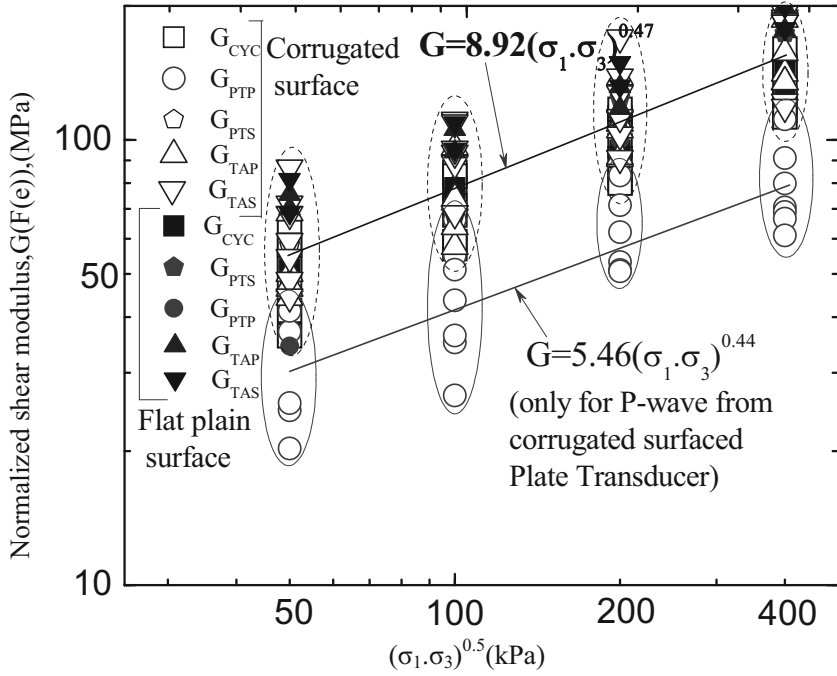


Figure 31. Results of Hime gravel in various conditions.

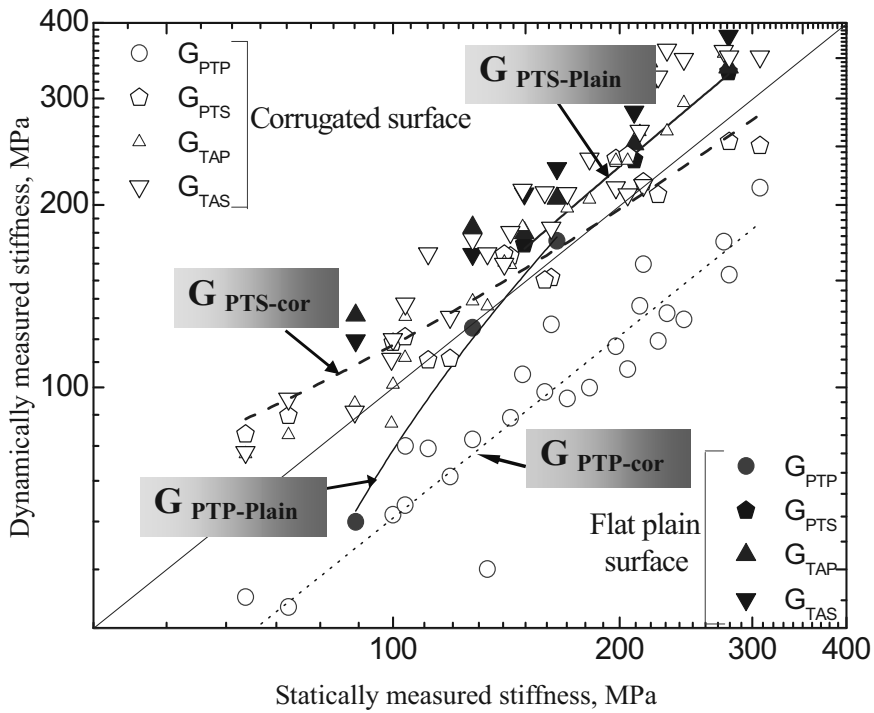


Figure 32. Comparison of dynamically and statically measured shear stiffness.

## CONCLUSION

The study to identify the effects of contact surface condition between tested materials and Plate Transducer in wave measurement was conducted. Corrugated surface and flat plain surface were mainly used in this study. There is bedding error at each interface and degree of errors seemed to be influenced by the condition of interfacing surface as well as the grain size of tested materials. Plain surface appeared to introduce less bedding error and give stable results compared to corrugated surface as long as voltage level of the received wave is sufficiently large. But, for looser specimen at lower stress levels, the measurement using plain surface was difficult. In such a case, it is recommended to secure good contact at interface by increasing surface area with respect to the grain size of the tested material.

## REFERENCES

1. De Silva, L.I.N. (2004), "Locally Measured Quasi-Elastic Deformation Properties of Geo-materials under Torsional Shear and Triaxial loadings", Master's degree Dissertation, The University of Tokyo.
2. Goto, S., Tatsuoka, F., Shibuya, S., Kim, Y-S., and Sato, T. (1991), "A simple Gauge for local small strain Measurements in the laboratory", *Soils and Foundations*, Vol.31, No.1, pp.169-180.
3. Hardin, B.O. and Richart, F.E. (1963), "Elastic wave velocities in Granular Soils", *Journal of Soil Mechanics and Foundations, ASCE*, Vol.89, No.1, pp.33-65.
4. Hoque, E., Tatsuoka, F. and Sato, T. (1996), "Measuring anisotropic elastic properties of sand using a large triaxial specimen", *Geotechnical testing journal, GTJODJ*, Vol.19, No.4, pp.411-420.
5. Kuwano, R., Wicaksono, R.I and Mulmi, S. (2008), "Small strain stiffness of coarse granular materials measured by wave propagation", *Proc. of 4th international symposium on deformation characteristics of geomaterials, IS-Atlanta 2008*, Vol.2, pp.749-756.
6. Mulmi, S., Kuwano, R. and Sato, T. (2008), "Performance of Plate-ceramic Transducers for Elastic Wave measurements in Laboratory Soil-specimens", *Seisan Kenkyu, Bimonthly Journal of Institute of Industrial Science, The University of Tokyo*, Vol.60, No.6, pp.565-569.
7. Suwal, L.P., and Kuwano, R. (2009), "Performance of Plate transducer, Transducer for dynamic measurement in Laboratory specimens", *Proc. of 11th international symposium, September 11, 2009, Tokyo, Japan, Japan Society of Civil Engineers*, pp.113-116
8. Suwal, L.P., and Kuwano, R. (2010), "Development of disc shaped pieze-ceramic plate transducer for elastic wave measurements in laboratory specimens", *Seisan-Kenkyu, Bimonthly Journal of Institute of Industrial Science, The University of Tokyo*, Vol.61, No.6, pp. 123-128
9. Tatsuoka, F. and Shibuya, S. (1991), "Deformation Characteristics of Soils and Rocks from Field and Laboratory Tests", *Keynote Lecture for Session No.1, Proceedings of the 9th Asian Regional Conference on SMFE, Bangkok, Thailand*, 2, pp.101-170.
10. Wicaksono, R.I, and Kuwano, R. (2009), "Small strain shear stiffness of Toyoura sand obtained from various wave measurement techniques", *Bulletin of Earthquake Resistant Structure Research Center, The university of Tokyo*, No.42, pp.107-119.